

# Signed Distance Based Reconstruction for Exploration and Change Detection in Underground Mining Disaster Prevention

Philipp Koch<sup>1</sup>, Helmut Engelhardt<sup>1</sup>, Stefan May<sup>1</sup>, Michael Schmidpeter<sup>1</sup>, Jasmin Ziegler<sup>1</sup> and Andreas Nüchter<sup>2</sup>

**Abstract**—This publication describes an application of a Truncated Signed Distance Mapping approach for disaster intervention in underground mine shafts through geometrical change detection of the shaft walls. The paper describes two main problems of such an approach (aligning two potentially huge point clouds and automatic change detection by comparing the reconstructed volumes) and explains in detail the proposed solution.

**Index Terms**—signed distance, stereo camera, underground mining, change detection

## I. INTRODUCTION

This Paper is an extension of already published work [1]. Underground mining is a lucrative, but dangerous business. With the increasing demand of raw substances, the number of mines world wide is rising steadily. Underground mine shafts are difficult to maintain and detecting potentially dangerous changes in the shaft conditions is complicated. Currently, the general approach is to send in human workers to inspect the shaft walls. In the vertical shafts, the men are placed on the pit cage and travel slowly down and up the shaft.

On the one hand, it is an inefficient waste of human work force, on the other hand, it is dangerous. The number of injuries in the mining business is rising with the number of mines world wide. Saving life is one very important aspect of automating the surveillance process. Another one, is efficiency. With increasing demand, production needs to be increased or at least be more efficient.

By replacing the human workers through an automated system, efficiency is increased. On one hand, human workers are way more expensive than machines, on the other, an automated system does not need breaks or vacation. Whenever the production is suspended, the system can do a measurement run, wherefore unexpected down times in the production can be used to check the shafts for cracks or similar.

## II. RELATED WORK

The base of the proposed approach is the well known Truncated Signed Distance (TSD) 3D representation. The approach was first introduced by Curless and Levoy [2]. Later, an accelerated version (KinectFusion) using one of the first consumer 3D sensors, the Microsoft Kinect camera, was published by Izadi et. al. [3] and Newcombe et. al. [4].

More applications using the TSD followed, i. e. Bleier et. al. [5].

Previously published work [6] ported the KinectFusion approach from a Graphic Processing Unit (GPU) based algorithm to a more energy efficient Central Processing Unit (CPU) algorithm.

Another problem which has been addressed in this paper is the memory consumption. A pure Voxel based approach allocates storage for the complete volume. Since most of the Voxel contain only free space, this memory is wasted. By dividing the room in partitions and allocating only space for non empty ones, only the necessary memory is allocated.

Another detail of the approach are the sensor models. In such a model, the physical properties of the input sensor is stored in mathematical methods. It also contains the pose from which the data was recorded and the actual data. With this approach, it is possible to fuse multiple sensor inputs even though the devices differ, into one map.

By removing a dimension, a 2D multi SLAM was created which is already published as an open source Robot Operating System (ROS) package and used within the RoboCup Rescue community ([7], [8]). This approach was used by Nüchter et. al. to localize a back pack based 3D SLAM system [9].

Many approaches on change detection are based on Gromov-Hausdorff distances e.g. ([10] [11]). The approach presented in this paper describes a different way to compare pointclouds. The dense TSD based representation is divided in slices and can be converted into 2d images and be compared step by step using basic image operations.

## III. SENSOR MODELS

The EU-funded project iDeepMon aimed at developing an inspection tool for vertical mine shafts. The system has been designed particularly for shafts, which contain a lift. The iDeepMon sensor system contains eight cameras to generate a panoramic view of the shaft while the lift moves up or down (scheme is shown in fig. 1). The idea behind this system is, to build a tool which can be used easily by trained mine inspectors to check the shaft for rust, water or other visually apparent damage. Figure 2b depicts the prototype in a mine in Sweden.

<sup>1</sup>Institute of Technology Georg-Simon-Ohm, Nuremberg

<sup>2</sup>Informatics VII : Robotics and Telematics, Würzburg

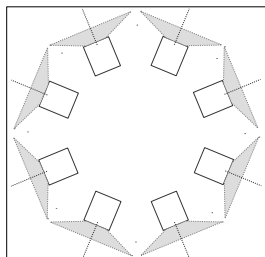


Fig. 1. Scheme of the iDeepmon prototype.

#### IV. DATA SOURCES

This approach was developed in the iDeepMon project. The german company DMT and the German Aerospace Center (DLR) have developed a mine shaft inspection tool called *Pilot* which uses a stereo camera and an Inertial Measurement Unit (IMU) to build 3D maps of underground shafts ([12]). The iDeepMon prototype contains such a system to improve the localization.

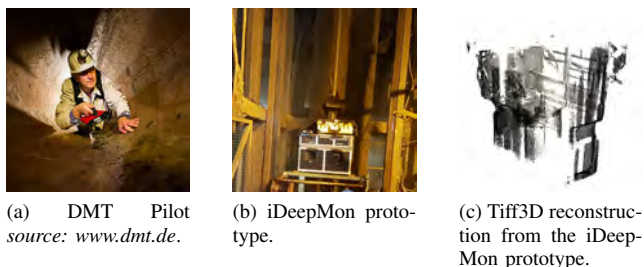


Fig. 2. Sensors for mineshaft reconstruction.

For inspection purposes and depth map generation, the prototype has eight overlapping cameras. The pictures are combined to panoramic images. Stereo images are generated using a structure from motion approach. Figure 2a shows the Pilot system, figure 2b shows the iDeepMon prototype in a working ore mine in Kristineberg, Sweden. Figure 2c shows a TSD reconstructed partial cloud from the shaft in Sweden.

The project had a quite difficult birth. After a feasibility study addressing numerous mining companies, the original sensor model (localization using an Inertial Measurement Unit (IMU) and odometer, volume reconstruction using two 2D laser scanners mounted below) had to be completely exchanged with an 8 camera system and localization using a hand held stereo camera device.

In the iDeepMon project, the Pilot system is integrated into the camera system to give a more accurate localization. Unfortunately, it is not possible to get raw data out of the pilot, because it calculates Simultaneous Localization and Mapping (SLAM) on the fly and the only output is a map and point clouds in the world coordinate system. As the sensor system was newly developed during the project, the pilot data was the only real data available for most of the project so the TSD framework needed to be adjusted in order to use

this data. So it is necessary to handle both data sources with the same priority.

#### A. Pilot

This setup has been developed with the German Aerospace Center (DLR) and is normally used to inspect difficult to access mine shafts, bunkers, ship hulls or similar. The project itself has been described by Benecke et. al. [12]. Figure 2a illustrates the device and shows, how to use it.

As already described in previous work ([6]), the TSD framework requires a sensor model with a mathematical description. In order to use it with the framework, a back projection approach is necessary as well as a Raycast model. As the pilot uses a stereo camera system, a pinhole camera model would be applied under normal circumstances. As the data is in point cloud format, a more generic approach needed to be found.

Following the original sensor concept (bottom mounted 2D laser scanner with 3D localization), the point cloud is divided in to slices as it would have been measured by a downward moving 2D laser scanner. The back projection approach addresses all Voxel in the representation, it works as follows.

The input point cloud is sorted into a data array, containing the slices similar to laser scans. The algorithm therefore has to calculate a slice index  $i_z$  and a beam index  $i_b$ . This tuple  $\vec{i} = (i_z, i_b)^T$  defines where the corresponding point  $\vec{p}_i$  out of the input cloud is mapped to. The calculation is straight forward and depicted in equations 2 and 1, where  $p_z$  is the  $z$ -coordinate of the corresponding point and  $s$  is the number of slices to calculate. Fig. 4a depicts how one slice of the array is calculated. The calculated index  $i$  is used to sort the corresponding point  $\vec{p}_i$  into the array  $\mathbf{D} = \{\|\vec{p}(i_z, i_b)\|\}$ .

Finally, the data is pushed into the representation. By applying equations 2 and 1 to the center of the current voxel, the corresponding array element  $i$  is determined. The signed distance is calculated using equation 3, with  $\vec{t}_i$  the current translation and  $\vec{v}_i$  the center of the current voxel. Figure 3a shows a raw point cloud input from the pilot, figure 3b the corresponding TSD reconstruction.

$$i_z = \frac{p_z}{s} \tag{1}$$

$$i_b = \frac{\text{atan2}\left(\frac{p_y}{p_x}\right)}{s} \tag{2}$$

$$d(\vec{v}) = D(i) - \|\vec{t}_i - \vec{v}_i\| \tag{3}$$

The sensor is completed with a Raycasting approach for reconstruction. For the cylindrical sensor model, rays are defined similar to a 2D laser scanner. The rays run in the  $x$ - $y$ -plain. Creating multiple slices along the  $z$ -axis completes the Raycasting model. Figure 3c depicts how the rays are calculated.

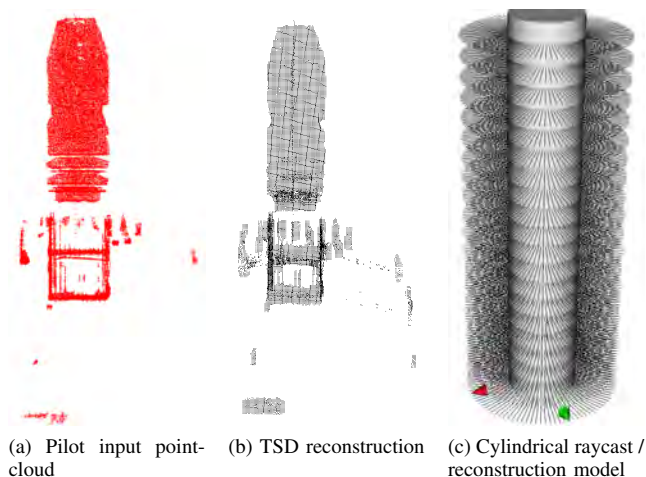


Fig. 3. TSD Reconstruction in the cylindrical model.

### B. Tiff3D, iDeepMon prototype

With the finalization of the sensor concept, a data structure for the recorded images and the estimated depth data was needed. The Tiff3d format contains color data, depth data as well as intrinsic and extrinsic data. The iDeepMon prototype records panoramic images and by estimating stereo features in images while moving downwards, 3D data is estimated. As the stereo matching is done for every single camera, the application the TSD framework is straight forward. Previous work ([6]) has already shown the capabilities of the framework with a pinhole based 3D camera. The application on the panoramic camera system is straight forward, as simply eight single instances are pushed one after another into the volume.

The same approach is applied to the Raycasting reconstruction. Instead of using a single sensor, the panoramic reconstruction is generated by repeating the Raycast from eight different poses and pushing the resulting point data into one point cloud. Figure 4b visualizes the Raycasting from one camera, figure 4c shows a panoramic reconstruction out of a TSD volume.

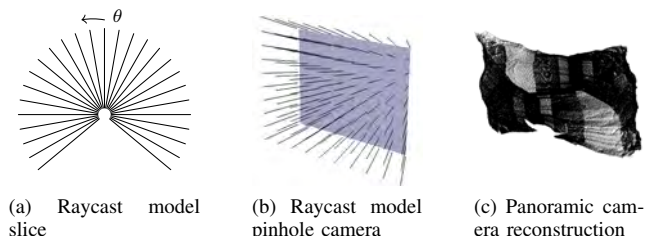


Fig. 4. Raycasting Models

## V. ALIGNMENT OF VOLUME RECONSTRUCTIONS

Volumetric change detection is performed, by comparing the 3D reconstructions of different measurement runs. By

repeating such runs in constant intervals, a change detection software can detect potentially small volumetric changes. Such changes can be signs of imminent disaster. In order to compare two reconstructed volumes, they need to be aligned first.

Small changes in the starting position and noise on localization or sensor data causes misalignment between the volumes which has to be corrected before. Therefore, an alignment procedure is required, which determines the error between both data sets. It consists of a Rotation Matrix  $\mathbf{R}_{3 \times 3}$  and a translation vector  $\vec{t}(x, y, z)^T$ , both combined in the transformation matrix  $\mathbf{T}_{4 \times 4}$ .

$$\mathbf{T} = \begin{pmatrix} \mathbf{R}_{00} & \mathbf{R}_{01} & \mathbf{R}_{02} & t_x \\ \mathbf{R}_{10} & \mathbf{R}_{11} & \mathbf{R}_{12} & t_y \\ \mathbf{R}_{20} & \mathbf{R}_{21} & \mathbf{R}_{22} & t_z \\ 0 & 0 & 0 & 1 \end{pmatrix}$$

Aligning potentially big point clouds is a difficult and expensive process, wherefore this publication proposes an iterative approach, exploiting the benefits of a TSD based representation. As its dense representation allows high resolution Raycasting, new sensor frames can be matched easily to an already existing model space.

Therefore, the described approach uses the input data with its localization for an iterative alignment. One of the major upsides of a TSD based reconstruction is its dense data structure, which allows high quality reconstruction via raycasting. This particular benefit is used to match new data not against the previous sensor frame but directly against the map which fuses all acquired measurements using a weighted average and is therefore virtually drift free. The main difference to approaches which use only the sensor input for matching is, that no drifting error is accumulated. The described approach has already been used in previous work, a 2D Multi SLAM approach ([7], [8]).

In iDeepMon, new sensor frames are tagged with a localization generated by a sensor system. In the following, the reference data is called *Modelspace* ( $\mathbf{M}$ ) and the to be matched data set *Scenespace* ( $\mathbf{S}$ ). To correct potential drift on the pose of the new scene data, it is matched against the already existing data of the Modelspace using Raycasting and a scanmatching approach.

The scene data is pushed from the corrected pose into the Scenespace, generating a drift corrected space which only contains the potentially dangerous volumetric changes which the second stage of the algorithm has to detect. Figure 5 shows the undistorted Modelspace, and the Scenespace with a simulated drift prior to alignment. The data used for this reconstruction has been provided by the DLR.

In order to align two big point clouds from different measurement campaigns, a similar approach as in the multi SLAM is applied. All sensor frames contain the measured data and a  $\mathbf{T}_{4 \times 4}$  transformation matrix:

To generate the modelspace, the data is simply pushed into a TSD volume. In order to reduce the drifting error, every



Fig. 5. TSD Shaft reconstructions before the alignment. Reference volume (left), drift afflicted measurement (right).

new frame is matched against the already generated volume.

An iteration of the alignment process starts with reconstructing the model data by using a sensor specific ray caster. This data, the model data  $M = \{\vec{m}_i \mid i = 1..n_m\}$ , is generated from the current position  $t_i$ , stored in the sensor frame. It contains coordinates  $\vec{m}_i = (x_i, y_i, z_i)^T$ . The sensor also contains the scene data from the measurement  $D = \{\vec{d}_i \mid i = 1..n_m\}$ .

The well known Iterative Closest Point (ICP) algorithm introduced by Zhang and Zhengyou [13] and Chen and Medioni [14] is used to match  $M$  and  $D$  against each other and the resulting transformation matrix  $T_*$  contains the drifting error. The sensor pose is corrected by applying  $T_*$  to its pose:

$$T_{i+1} = T_*^{-1} * T_i \quad (4)$$

## VI. CHANGE DETECTION

The algorithm proposed in this approach exploits the benefits of the TSD based representation. The TSD-function can be transformed into a 2D image by coloring the referring pixel according to the value and sign of the TSD function in a slice of the representation. While this approach works for all dimensions, the proposed algorithm uses slices along the z-axis.

The image is generated by reading by iterating over the slice Voxel by Voxel and reading the contained TSD value. In order to depict the sign change, red and blue colors are used. Red corresponds to negative, blue to positive signs (see figure 6). As the value of the TSD is in a range of  $||[-1.0, 1.0]||$  and the zero transition is the most important to see, the lowest TSD value corresponds to the brightest color. By comparing two spaces slice by slice, even small changes can be detected and localized using methods of image processing e.g. thresholding.

The so generated difference images are converted back into a point cloud. To localize the changes, a clustering

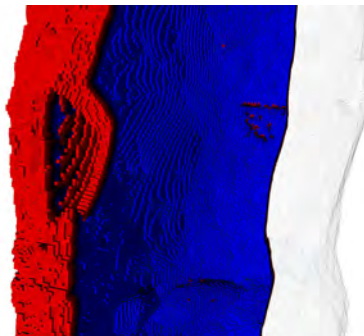


Fig. 6. Reconstructed pointcloud with marked change

approach and a principal component analysis implementation generate bounding boxes. Figure 7a shows z-slice taken from the Modelspace. Figure 7b shows the corresponding scene slice with a marked change.

Figure 6 depicts a 3D reconstruction of a TSD space with marked (dark) change in the point cloud and estimated bounding box.

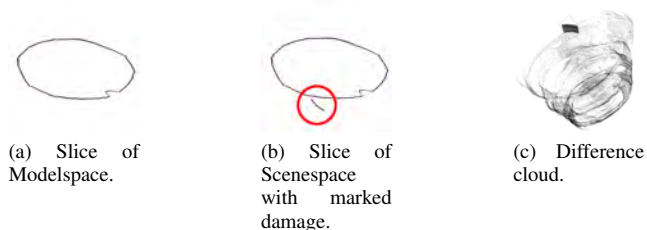


Fig. 7. Slice comparison.

## VII. EXPERIMENTS

### A. Pilot data

At the current project stage, the DMT pilot is the only available data source. A measurement run from top to bottom and back contains a significant drift ((x, y)-axis approximately 5m ). The TSD volume is able to correct this drift so the top to bottom measurement run can be compared to the bottom to top. The main problem of the iDeepMon project was, that the hardware changed completely after the feasibility study in the beginning. The point clouds recorded by the pilot in Reichenzeche was the only available real data source. The change detection approach requires at least two data sets, preferable from two different dates. The measurement with the pilot contained a path downwards and upwards which contained a significant drift which caused a misalignment between the point clouds.

In order to test the cylindrical sensor model and the alignment approach, these two point clouds consisting of around 122 m shaft length where aligned.

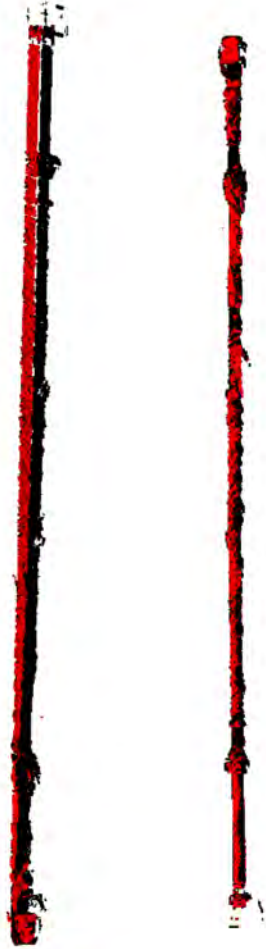


Fig. 8. TSD volumes before (left) and after alignment (right)

Image 8 shows both reconstructed point clouds before and after alignment. Image 9 shows the starting point which contained the most drift aligned in detail. This experiment showed, that the cylindrical model can be used to reconstruct a TSD volume from point cloud data. It also depicts, that the alignment of the spaces is possible with the approach.

*B. Simulated Tiff3D data*

The DLR provides simulated Tiff3D data. The reconstructed shaft is twisted and elongated using a simulated random drift. The threshold for the random data is increased in every stage of the algorithm to evaluate the capabilities of the alignment algorithm. The data of the iDeepMon prototype will be provided in Tiff3D format. As already mentioned, the only usable data, is simulated from the DLR. This data has been used in order to test the alignment with a simulated drift as well as the change detection with simulated deformation.



Fig. 9. End of shafts before (left) and after alignment (right)

For the alignment, the worst case has been simulated. The algorithm adds a random value to the rotation around the z-axis yaw angle and translation. To simulate the worst case, the error is been added in every iteration with positive values so with increasing depth, the shaft gets twisted and elongated. The approach therefore has to compensate this simulated error. The drift simulation takes a random value from 0 to  $x$  with  $x$  being an adjustable parameter.

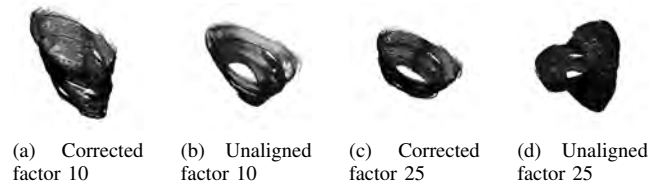


Fig. 10. Experimental space alignment with increasing simulated drift.

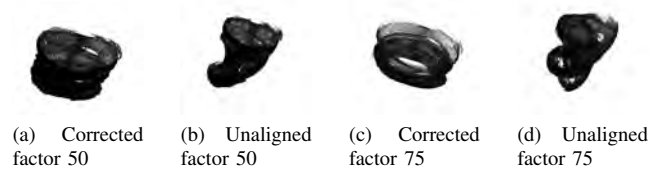


Fig. 11. Experimental space alignment with increasing simulated drift.

The figures 10a, 10b, 11a, 11b, 11c and 11d depict the experiment. The random drift values are added between each panoramic tiff3D sensor frame. Images 12a and 12b illustrate the currently highest shaft distortion, the approach can still correct.

*C. Change Detection*

In order to test the change detection, a partial area in the simulated Tiff3D data is shifted geometrically. In order to test the capabilities of the change detection, the size of the area

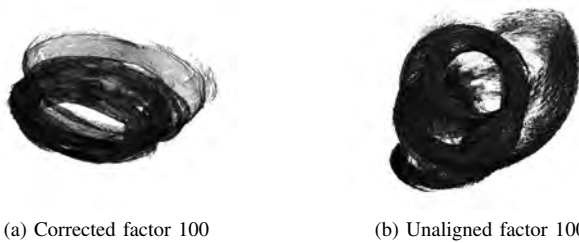


Fig. 12. Experimental space alignment with increasing simulated drift.

is decreased in every step of the experiment. In order to test this part of the approach, a simulated deformation has been added to the Tiff3D data. The generated TSD volume was compared to a damage free reference space and visualized with a bounding box. This experiment was performed with the simulated tiff3D data from the DLR.

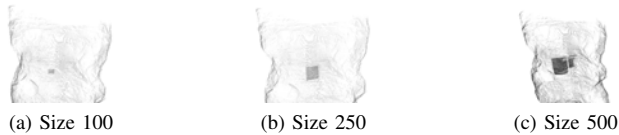


Fig. 13. Change detection example.

The figures 13a, 13b and 13c show the results of this experiment. While creating the Scenamespace, a part of the input tiff is pushed back and therefore creates an artificial hole the algorithm has to detect. The figures show, how the test decreases the size of the deformation in order to test the capabilities of the approach.

### VIII. CONCLUSION

In this paper, we presented a novel application for a TSD based 3D reconstruction. By exploiting the special design features of this representation, we created an application which can be used for disaster intervention vertical mineshafts. We provided experiments which showed the capabilities of the approach.

However, most experiments have been done with simulated data or the wrong sensor. Therefore, in future work, the approach has to be tested with data from the iDeepMon prototype. In order to get more data, new sensor interfaces will be developed to integrate point data from other existing shaft measurement systems.

### ACKNOWLEDGMENT

This work has been funded by EIT Raw Materials and was part of the EU Project iDeepMon.

This project uses the point cloud library:  
 (<http://www.pointclouds.org/>).



### REFERENCES

- [1] P. Koch, S. May, H. Engelhardt, J. Ziegler, and A. Nchter, "Signed distance based reconstruction for exploration and change detection in underground mining disaster prevention," in *2019 IEEE International Symposium on Safety, Security, and Rescue Robotics (SSRR)*, pp. 1–2, 2019.
- [2] B. Curless and M. Levoy, "A volumetric method for building complex models from range images," in *Proceedings of the 23rd Annual Conference on Computer Graphics and Interactive Techniques, SIGGRAPH '96*, (New York, NY, USA), pp. 303–312, ACM, 1996.
- [3] R. A. Newcombe, S. Izadi, O. Hilliges, D. Molyneaux, D. Kim, A. J. Davison, P. Kohli, J. Shotton, S. Hodges, and A. Fitzgibbon, "Kinectfusion: Real-time dense surface mapping and tracking," in *Mixed and Augmented Reality (ISMAR), 2011 10th IEEE International Symposium on*, pp. 127–136, Oct 2011.
- [4] S. Izadi, D. Kim, O. Hilliges, D. Molyneaux, R. Newcombe, P. Kohli, J. Shotton, S. Hodges, D. Freeman, A. Davison, and A. Fitzgibbon, "Kinectfusion: Real-time 3d reconstruction and interaction using a moving depth camera," in *Proceedings of the 24th Annual ACM Symposium on User Interface Software and Technology, UIST '11*, (New York, NY, USA), pp. 559–568, ACM, 2011.
- [5] M. Bleier, A. Dias, A. Ferreira, J. Pidgeon, J. M. Almeida, E. Silva, K. Schilling, and A. Nchter, "Signed Distance Function Based Surface Reconstruction of a Submerged Inland Mine Using Continuous-Time SLAM," in *Proceedings of the 20th World Congress of the International Federation of Automatic Control (IFAC WC '17)*, (Toulouse, France), July 2017.
- [6] S. May, P. Koch, R. Koch, C. Merkl, C. Pfitzner, and A. Nchter, "A generalized 2d and 3d multi-sensor data integration approach based on signed distance functions for multi-modal robotic mapping," in *VMV 2014: Vision, Modeling & Visualization, Darmstadt, Germany, 2014. Proceedings*, pp. 95–102, 2014.
- [7] P. Koch, S. May, M. Schmidpeter, M. Kuhn, C. Pfitzner, C. Merkl, R. Koch, M. Fees, J. Martin, and A. Nchter, "Multi-robot localization and mapping based on signed distance functions," in *Autonomous Robot Systems and Competitions (ICARSC), 2015 IEEE International Conference on*, pp. 77–82, April 2015.
- [8] P. Koch, S. May, M. Schmidpeter, M. Kühn, C. Pfitzner, C. Merkl, R. Koch, M. Fees, J. Martin, D. Ammon, and A. Nchter, "Multi-robot localization and mapping based on signed distance functions," *Journal of Intelligent & Robotic Systems*, vol. 83, pp. 409–428, Sep 2016.
- [9] A. Nchter, D. Borrmann, P. Koch, M. Kuhn, and S. May, "A man-portable, imu-free mobile mapping," in *Proceedings of the ISPRS Geospatial Week 2015, Laserscanning 2015*, ISPRS Annals Photogrammetry and Remote Sensing, Spatial Inf. Sci., II-3/W5, (La Grande Motte, France), pp. 17–23, September 2015.
- [10] F. Méoli and G. Sapiro, "Comparing point clouds," *ACM International Conference Proceeding Series*, vol. 71, no. January 2004, pp. 32–40, 2004.
- [11] D. Girardeau-Montaut, M. Roux, R. Marc, and G. Thibault, "Change detection on points cloud data acquired with a ground laser scanner," *International Archives of the Photogrammetry, Remote Sensing and Spatial Information Sciences - ISPRS Archives*, vol. 36, 2005.
- [12] N. Benecke, A. Born, A. Börner, S. Rapp, P. Stelzer, N. Tsigotis, M. Weber, and S. Zuev, "Mobile solution for positioning, 3d-mapping and inspection in underground mining," in *ISM2016, XVI International Congress for Mine Surveying*, April 2016.
- [13] Z. Zhang, "Iterative point matching for registration of free-form curves and surfaces," *Int. J. Comput. Vision*, vol. 13, pp. 119–152, Oct. 1994.
- [14] Y. Chen and G. Medioni, "Object modeling by registration of multiple range images," in *Robotics and Automation, 1991. Proceedings., 1991 IEEE International Conference on*, pp. 2724–2729 vol.3, Apr 1991.